Med Chem Res
DOI 10.1007/s00044-017-1891-0

MEDICINAL CHEMISTRY RESEARCH

ORIGINAL RESEARCH

Synthesis and biological evaluation of α-methyl-chalcone for anti-cervical cancer activity

Bing-zhao Ren[1] · Mourboul Ablise[1] · Xu-chao Yang[1] · Bo-er Liao[1] · Zheng Yang[1]

Received: 29 November 2016 / Accepted: 4 April 2017

Abstract A series of 31 chalcones were synthesized and evaluated for anti-proliferative activity against the human cervical cancer cell lines (HeLa and SiHa). Compound **19**, (E)-1-(2,4-dihydroxyphenyl)-3-(4-(dimethylamino) phenyl)-2-methylprop-2-en-1-one was found to be an effective anti-proliferative agent in HeLa and SiHa cells (IC_{50} = 0.035 μM). Compound **19** increased the percentage of apoptosis in a dose-dependent manner, as measured by Annexin V-FITC (fluorescein isothiocyanate)/(propidium iodide) PI staining. Molecular modeling studies of compound **19** showed that the most potent structure was docked at the yeast 20 S proteasome binding site (Protein Data Bank code-3E47) and was stabilized in the cavity by various hydrophobic and hydrogen bonding interactions.

Keywords Chalcone · α,β-Unsaturated · Carbonyl · Anti-cervical cancer molecular modeling · Anti-mitotic · Synthesis

Introduction

The ubiquitin-proteasome system is one of the major pathways of intracellular protein degradation, playing a prominent role in signal transduction, cell death, immune response, cell cycle regulation, metabolism, and protein expression. It is the 26S proteasome that completes ATP-dependent ubiquitin protein degradation (Tanaka 2009). The 26S proteasome is composed of one 20S catalytic subunit, which is known as the "proteolytic core" and two 19S regulatory subunits, which are termed "caps" (Ciechanover et al. 1984; Ciechanover 1993). The 20S proteasome contains fourteen α subunits and fourteen β subunits. Each β subunit is composed of three catalytic sites: β_1 (caspase-like), β_2 (trypsin-like), β_5 (chymotrypsin-like). The proteolytic activities of three subunits use the γ-hydroxyl group of an N-terminal threonine residue within each catalytic site for nucleophilic attack of the α-amine proton donor/acceptor within the targeted protein (Bazzaro et al. 2008).

Chalcones are naturally occurring compounds that are widely distributed in a variety of plant species belonging to the flavonoid family. They are known to exhibit several biological activities (Zhao et al. 2005; Valla et al. 2006; Lawrence et al. 2006; Hsu et al. 2006; Ahmad et al. 2006; Dimmock et al. 1999; Ni et al. 2005), including antiplatelet activity, inhibition of pro-inflammatory mediators, anti-proliferative action in cancer cells, apoptosis induction, antimalarial activity, and others. The method of synthesis of chalcones is mainly the Claisen—Schmidt condensation reaction, with a basic catalyst, such as NaOH (Romagnoli et al. 2009; Robert and Jarry 2003; Ahmed Belkacem et al. 2006), KOH (Zamora et al. 1988), and Ba(OH)2 (Lee et al. 1994; Liu et al. 2008), acetophenones, and benzene formaldehyde dehydration condensation. Other basic catalysts such as magnesium tert-butoxide (Lawrence and McGown 2005), K_2CO_3, Al_2O_3 (Seelig and Landwojtowicz 2000), MgO (Ducki et al. 1998), calcined hydrotalcites (Bois et al. 1998, 1999), the natural phosphate/$NaNO_3$ (Pati et al. 2005; Xia et al. 2000), the natural phosphate/KF (Dimmock et al.

Electronic supplementary material The online version of this article (doi:10.1007/s00044-017-1891-0) contains supplementary material, which is available to authorized users.

✉ Mourboul Ablise
mourboul@sohu.com

[1] Institute of Pharmacy, Xinjiang Medical University, Urumchi, China

Published online: 22 April 2017

2003) and piperidine (Liu and Go 2006) are also often used for the synthesis of chalcones. The reaction can also use an acid catalyst such as HCl, BF_3, B_2O_3, PTSA, $SOCl_2$/EtOH, BF_3–Et_2O (Petrov et al. 2008), $TiCl_4$ (Sogawa et al. 1993), Zeolite (Chimenti et al. 2005), and $RuCl_3$ (Climent et al. 1990). However, these catalysts have varying degrees of shortcomings, such as low yield and harsh reaction conditions, or are harmful to the environment. Microwave reactors have high yield, simple operation and post-processing (Iranpoor and Kazemi 1998; Deka and Sarma 2001; Kalita et al. 1999; Saikia et al. 2009).

Groll et al. 2006 reported a crystallographic analysis of the yeast 20 s proteasome in complex with the inhibitor homobelactosin C. Catalytic activities of these β-type subunits are associated with their N-terminal threonine residue, which acts as the nucleophile in hydrolysis, thus classifying proteasomes as members of the family of N-terminal nucleophilic hydrolases (Löwe et al. 1995; Brannigan et al. 1995). The 20 s proteasome subunits utilize the hydroxyl group of an N-terminal theronine within each catalytic site for nucleophilic attack of the carbonyl group of homobelactosin C, which leads inactivation of the proteasome. The α,β-unsaturated carbonyl system is the activity group of chalcone-based derivatives that inhibits proteasome activity in human papilloma virus-positive cervical cancer cells (Bazzaro et al. 2011).

Results and discussion

Chemistry

The chalcones were classified into 4 groups according to their substitution patterns on ring A and ring B (i.e., their 1-phenyl moiety). Group 1 chalcones (**1–4**) have no ring A substitution and ring B is substituted with a hydroxyl group at one position; Group 2 chalcones (**5–9**) are isoliquiritigenin derivatives; Group 3 chalcones (**10–16**) are fluorine isoliquiritigenin derivatives, and Group 4 chalcones (**17–31**) are α-methyl-chalcone derivatives. All synthetic compounds (Table 1) had satisfactory analysis and spectral data, which were completely described by their structure.

Biological activity

Anti-proliferation assay

The methyl thiazolyl tetrazolium (MTT) assay system was used to identify compounds with anti-proliferative activity. Human cervical cancer cells (HeLa and SiHa), normal Chinese Hamster Ovary (CHO) were incubated for 24 h/48 h/72 h at 37 °C. Table 2 lists the IC_{50} values of the chalcones for each cell line.

Compounds **2–9**, having electron donating groups, exhibited anti-proliferative activity. Notably, the target compounds of isoliquiritigenin derivatives showed dose-dependent and time-dependent growth inhibition in SiHa cells and HeLa cells. The isoliquiritigenins with an $–OCH_3$ group in the meta-positions on aromatic ring B were selectively anti-proliferative in SiHa cells, due to their increased lipid solubility, which caused greater penetration into the cells. Hydroxyl group substitutions in chalcones have been shown to play a key role in anti-cancer activities of chalcones. The isoliquiritigenin with –OH groups in the meta-positions and in the ortho-positions on the aromatic ring B induced a lower degree of growth inhibition than those without –OH groups. Thus, the $–OCH_3$ and –OH groups are important in influencing selectivity and potency of chalcone derivatives.

Compounds **10–16**, bearing –F on their A-rings and B-rings were initially synthesized and evaluated in terms of their activity. Those with an electron withdrawing group exhibited greater cytotoxic activity, and the cytotoxic activities of these compounds were related to the electrophilic nature of their substituent. For example, the IC_{50} value of compound **11** was 3.35 μM.

Comparisons were made to determine the effect of having a methyl group in the α position and another substituent (–OH, $–NO_3$, –F, $–N(CH_3)_2$, $–OCH_3$) on rings A and B (chalcones **17–31**). Chalcones **17–31** showed the most potent anti-proliferative effect against HeLa and SiHa cells, indicating that the methyl group on α position plays an important role.

Chalcone **19** exhibited the most potent anti-proliferative effect against SiHa cells with lowest IC_{50} (0.035 μM). Morphological changes (Fig. 1) show that chalcone **19** exhibited a greater growth inhibitory rate in SiHa cells at all concentrations than in HeLa cells. The anti-proliferative effects exhibited by chalcone **19** were also dose-dependent. From the photos (Fig. 1), it looks like cisplatin is more potent than compound **19** against cancer cells. In non-cancerous cells, cisplatin killed more cells than compound **19**. This could be interpreted as better selectivity of compound **19** for cancer cells than cisplatin and that it would be investigated further. Figure 2 shows that compound **19** displayed the highest anti-proliferative activity and therefore was chosen for further investigation. All growth inhibitory effects induced by chalcones were significantly different ($p < 0.05$) as compared with cells treated with 1% DMSO.

Apoptosis assay

Apoptosis is an essential mechanism used to eliminate activated cells during the shut down process of excess immune responses and to maintain proper immune

Table 1 Chalcone derivatives and their melting points

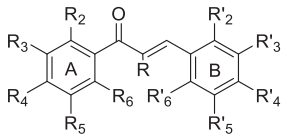

	Chalcone ring A						Ring B					
No.	R_2	R_3	R_4	R_5	R_6	R	R'_2	R'_3	R'_4	R'_5	R'_6	MP °C
1	H	H	H	H	H	H	H	H	H	H	H	55–56
2	H	H	H	H	H	H	OH	H	H	H	H	149–151
3	H	H	H	H	H	H	H	OH	H	H	H	223–224
4	H	H	H	H	H	H	H	H	OH	H	H	159–161
5	OH	H	OH	H	H	H	H	H	OH	H	H	198–200
6	OH	H	OH	H	H	H	H	OCH_3	OH	H	H	207–209
7	H	H	OH	H	H	H	H	OH	OCH_3	H	H	198–203
8	OH	H	OH	H	H	H	H	OH	OH	H	H	220–221
9	H	H	OH	H	H	H	H	H	OH	H	H	196–198
10	F	H	F	H	H	H	H	H	F	H	H	103–105
11	OH	H	OH	H	H	H	H	H	F	H	H	108–109
12	H	H	OH	H	H	H	H	H	F	H	H	104–105
13	OH	H	H	H	H	H	H	H	F	H	H	106–107
14	F	H	F	H	H	H	H	H	OH	H	H	105–107
15	F	H	F	H	H	H	H	OCH_3	OH	H	H	110–111
16	F	H	F	H	H	H	H	OH	OCH_3	H	H	110–112
17	OH	H	OH	H	H	CH_3	H	H	NO_2	H	H	163–164
18	OH	H	OH	H	H	CH_3	H	H	F	H	H	176–178
19	OH	H	OH	H	H	CH_3	H	H	$N(CH_3)_2$	H	H	89–92
20	OH	H	OH	H	H	CH_3	H	H	H	H	H	113–115
21	OH	H	OH	H	H	CH_3	H	OCH_3	OH	H	H	103–105
22	H	H	H	H	H	CH_3	H	H	NO_2	H	H	103–105
23	H	H	H	H	H	CH_3	H	H	F	H	H	100–102
24	H	H	H	H	H	CH_3	H	H	$N(CH_3)_2$	H	H	85–87
25	H	H	H	H	H	CH_3	H	H	H	H	H	115–117
26	H	H	H	H	H	CH_3	H	OCH_3	OH	H	H	95–97
27	H	H	OH	H	H	CH_3	H	H	NO_2	H	H	91–93
28	H	H	OH	H	H	CH_3	H	H	F	H	H	90–93
29	H	H	OH	H	H	CH_3	H	H	$N(CH_3)_2$	H	H	121-123
30	H	H	OH	H	H	CH_3	H	H	H	H	H	92–93
31	H	H	OH	H	H	CH_3	H	OCH_3	OH	H	H	123–125

homeostasis, while deficient apoptosis of activated cells is associated with a wide variety of immune disorders. As a representative of the chalcone thiosemicarbazide derivatives, compound **19** was further evaluated for its apoptotic effect. We assessed the mechanism underlying the cell growth inhibition by compound **19** by flow cytometry in SiHa and HeLa cells following a 24 h treatment with 0.01, 0.1, 1, 6.25, 12.5 μg mL^{-1} of compound **19**. The compound increased the percentage of apoptosis in both cell lines, as revealed by Annexin V-FITC/PI staining, in a dose-dependent manner (Figs 3 and 4).

Molecular docking simulation

In order to obtain a deeper insight into the molecular basis of the enzyme-inhibitor recognition process, docking simulation of the most active (compound **19**) was performed to investigate its binding mode to the 20S proteasome that is co-crystallized with the β5-inhibitor, homobelactosin

Table 2 The anti-proliferative effects of chalcones for cancer cells and CHO cells

Chalcone no.	HeLa IC_{50} μM			SiHa IC_{50} μM			CHO IC_{50} μM		
	24 h	48 h	72 h	24 h	48 h	72 h	24 h	48 h	72 h
1	>100	>100	>100	>100	>100	>100	>100	98.21	89.27
2	67.21	60.74	45.05	66.82	63.01	52.2	97.66	80.33	75.23
3	70.45	65.34	61.87	74.23	68.67	62.3	40.32	35.56	23.71
4	>100	76.81	63.72	>100	80.53	75.6	51.23	45.65	32.71
5	31.01	23.92	19.75	29.21	23.61	18.41	55.12	43.57	27.42
6	46.34	34.6	23.38	38.14	25.34	21.63	60.87	53.45	38.27
7	48.03	31.57	16.78	46.1	44.25	33.6	59.36	47.51	40.03
8	62.4	29.43	6.87	75.21	1.74	0.182	56.15	48.35	38.76
9	17.72	14.56	13.13	34.97	14.81	6.89	48.69	45.68	32.11
10	42.54	23.66	19.75	23.32	16.72	10.23	49.36	47.23	35.12
11	40.34	32.67	10.25	15.54	10.43	3.35	48.71	44.36	31.56
12	39.34	26.57	15.65	25.21	16.54	12.76	45.63	38.52	33.28
13	34.44	27.43	16.57	17.67	12.87	5.02	47.64	40.66	34.75
14	27.25	19.44	12.43	16.97	12.48	8.1	40.36	35.36	28.57
15	38.45	30.23	20.56	22.54	15.67	10.79	43.81	37.83	29.49
16	39.65	16.94	14.56	22	15.76	5.87	41.86	37.92	30.01
17	10.43	6.5	0.231	5.11	2.12	0.187	47.56	40.42	31.2
18	13.35	6.22	2.34	5.35	8.48	0.673	50.94	45.36	34.75
19	10.45	4.45	0.082	4.35	1.01	0.035	54.68	47.55	38.49
20	17.04	5.56	0.56	4.24	3.46	0.178	55.11	48.21	37.14
21	13.32	8.76	2.53	6.32	1.34	0.105	56.47	46.38	37.08
22	20.15	10.11	2.54	10.53	2.65	1.36	59.46	45.55	38.33
23	23.65	15.23	1.65	16.54	4.31	2.03	63.45	59.46	40.59
24	19.84	11.58	1.11	14.13	1.85	0.94	57.31	48.54	40.91
25	25.98	16.42	1.84	18.36	6.31	3.12	58.64	49.59	34.31
26	17.56	17.22	0.912	23.54	5.24	2.41	48.31	36.89	32.66
27	25.61	11.03	0.847	23.12	6.17	1.34	57.13	52.81	45.76
28	19.58	13.23	1.035	17.64	8.23	2.13	41.36	39.46	37.21
29	18.66	9.55	2.156	19.71	5.46	5.79	39.45	38.23	36.32
30	25.98	6.89	1.65	18.54	5.24	6.85	37.64	23.16	20.36
31	20.36	14.63	2.360	17.64	3.85	4.31	49.15	45.63	42.34

C. Structures were retrieved from the Protein Data Bank, PDB (Rocco et al. 2006). Compound **19** was docked at the homobelactosin C binding site of the yeast 20S proteasome (**a**, **b** in Fig. 5a) and the best fit conformation was selected on the basis of the Gold score and visual inspection.

The docking study showed that compound **19** is stabilized in the 20S proteasome by hydrogen bonding and hydrophobic interactions. Many of the amino acid residues, which are in the formation of the ligand-binding pocket, i.e., THR1, THR21, GLY47, and SER129, formed H-bonds with hydroxyl and carbonyl groups of compound **19**. The oxygen atom of the para-hydroxyl group of ring A acts as an H-bond acceptor and is involved with chain NH of THR-21 ($d = 2.9$ Å). The carbonyl group of α,β-unsaturated carbonyl system was located 2.7 Å away from the nucleophilic serine residue (SER-129), a distance that is typical of a hydrogen bonding interaction in this type of emulation with a rigid protein frame. Figure 5 shows that additional but weak H-bonds were also observed between compound **19** and other amino acid residues (d = 2.7–3.2 Å). The dimethylamino group of compound **19** is extended toward the β subunits of the ligand-binding pocket positioned in a hydrophobic cavity formed by Gly47 and Gly98. The molecular docking studies suggest a nucleophilic attack from the N-terminal threonine residue of the β-subunits to the carbonyl group of compound **19** as a mechanism for proteasomal inhibition.

Conclusion

A series of chalcone derivatives containing electron-withdrawing and electron-donating substituents have been

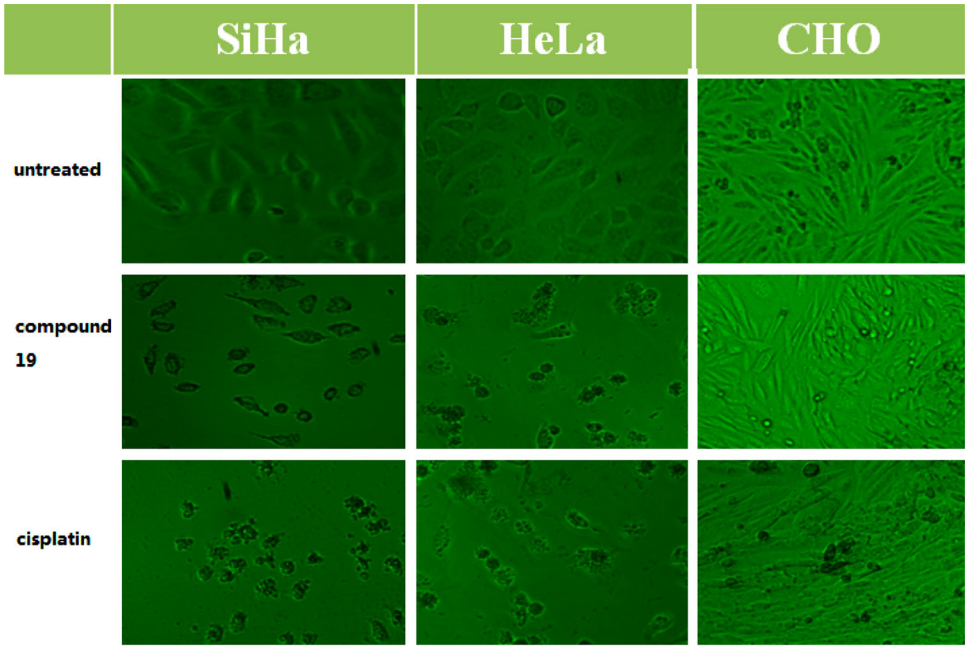

Fig. 1 The morphological changes of human cervical cancer and CHO cells with compound **19**

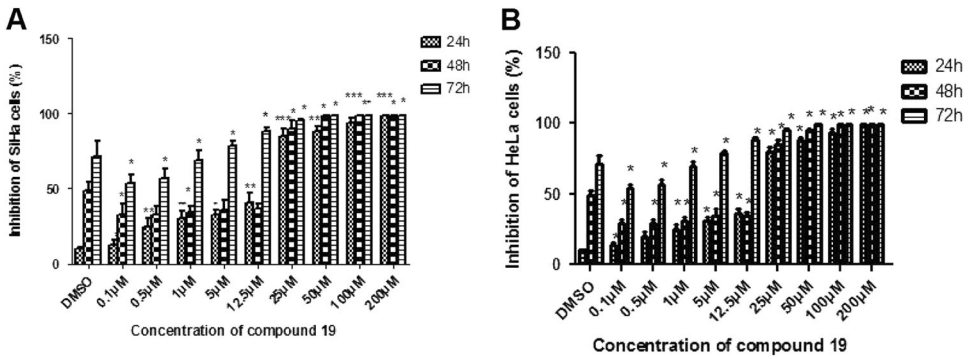

Fig. 2 Inhibition rate of compound **19** toward SiHa **a** and HeLa **b** cells after 24, 48 and 72 h

designed and synthesized and their biological activities were also evaluated as potent and selective anti-proliferative activity against human cervical cancer cells (SiHa and HeLa). Chalcone **19** showed the most potent growth inhibitory activity toward SiHa and HeLa cells with IC_{50} values of 0.035 and 0.082 μM, which was slightly lower than the positive control (cisplatin), and ideal quality of a potential cancer drug—low toxicity to normal tissue with IC_{50} value of 38.49 μM toward CHO cells, which was obviously higher than cisplatin.

Experimental

Chemistry

All of the solvents and reagents used in the current study were purchased from commercial suppliers and used without further purification. Melting points were recorded on an X-4 melting point apparatus and are uncorrected. Thin layer chromatography (TLC) analysis was done using silica gel 60 F254 analytical plates (Merck, Billerica, MA, USA). The reaction products were purified by crystallization or flash column chromatography using a mixture of petroleum ether/ethyl acetate and hexane/ethyl acetate as the eluent. FT-IR spectra were carried out on Bruker RFS100/S spectrophotometer (Bio-Rad, Cambridge, MA, USA) in the 400–4000 cm^{-1} range. 1H-NMR spectra were recorded on Varian Inova-600 MHz instruments (Varian, Palo Alto, CA, USA). 13C-NMR spectra were recorded on a 600 MHz Bruker ARX-600 spectrometer (Bruker Bioscience, Billerica, MA, USA). The chemical shifts (δ) are reported in parts per million downfield relative to tetramethylsilane. All tested compounds were >95% purity as determined by preparative TLC, which was made using silica gel GF254 on glass plates. The chalcones were prepared according to methods previously described in the literature (Leong et al. 2007, 2005; Rocco et al. 2006).

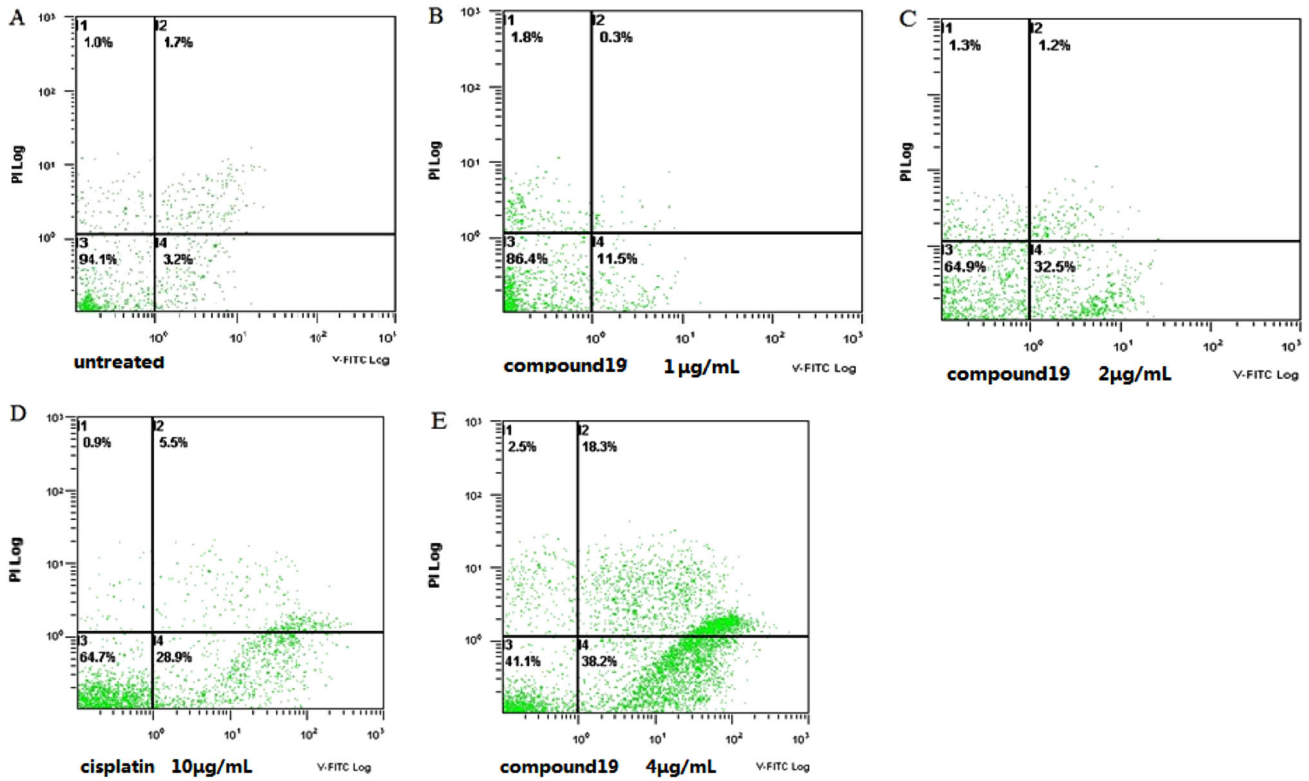

Fig. 3 The apoptotic effect of compound **19** in SiHa cells

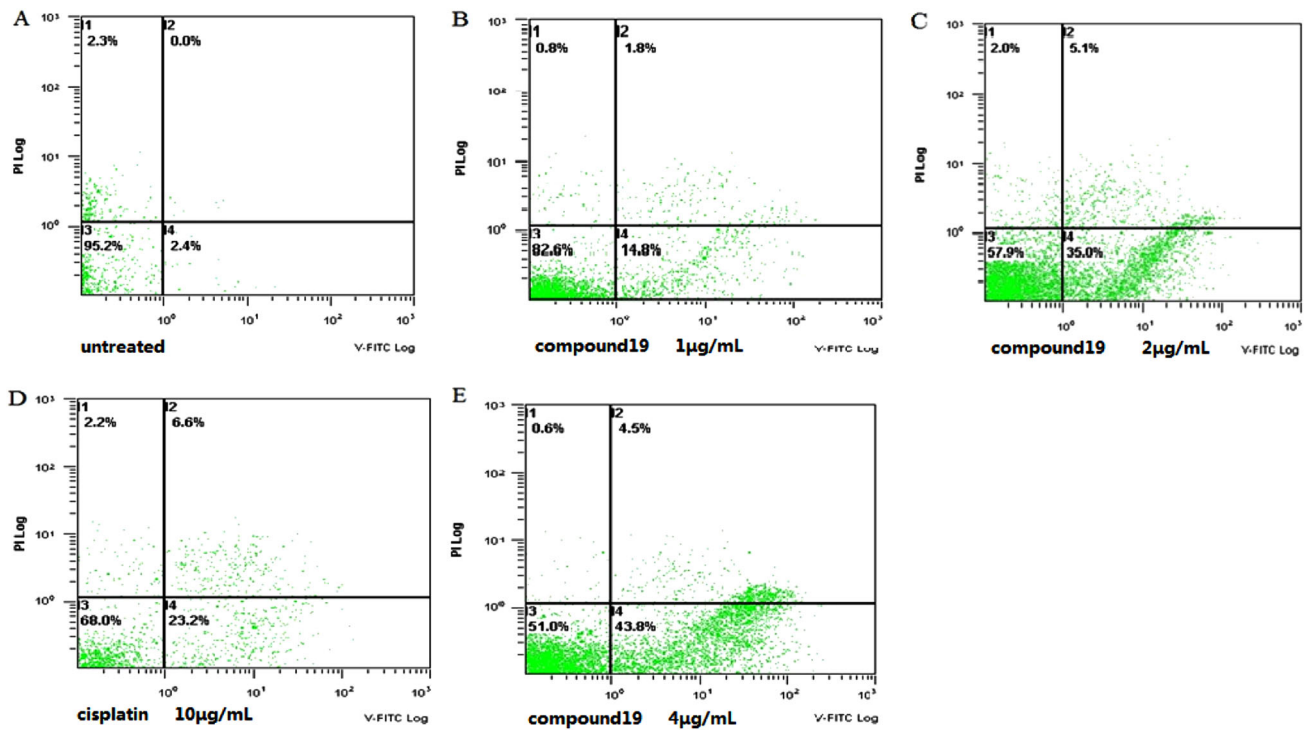

Fig. 4 The apoptotic effect of compound **19** in HeLa cells

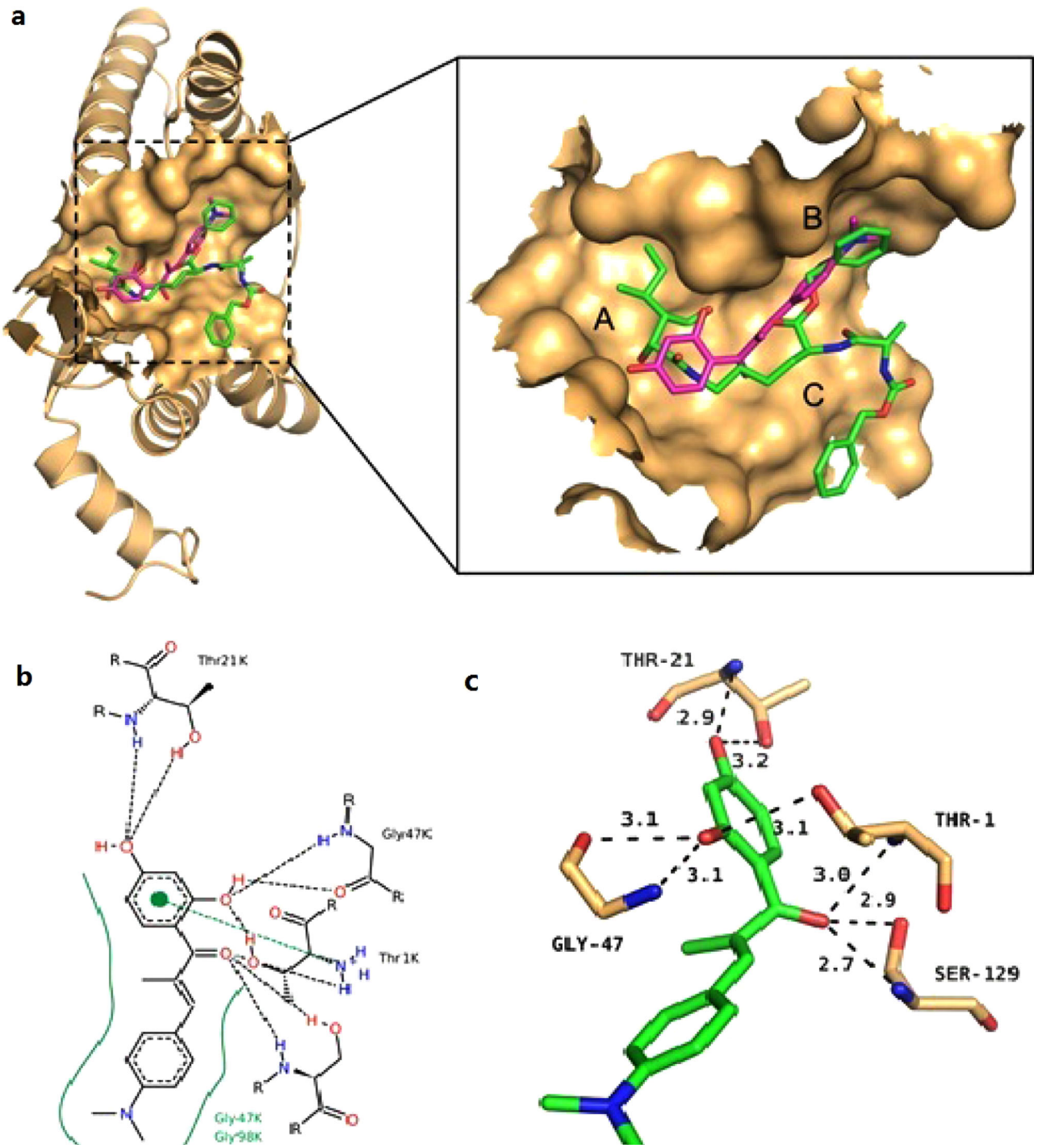

Fig.5 Docking simulation of lead compound **19** to the 20S proteasome. **a** Compound **19** (*red*) and the ligand of proteasome (*green*) are binding at the A, B, and C active sites. **b** and **c** Schematic view of lead compound 19 (*green*) docked to the crystal structure of the 20S proteasome (color figure online)

General methods for chalcones ***2–9***

The chalcones (**2–9**) evaluated in the current study were synthesized by the base catalyzed Claisen–Schmidt condensation reaction of the appropriately substituted acetophenones and aldehydes (Scheme 1). The chalcones prepared according to this method were formed predominantly with the (E)-configuration.

Acetophenones (0.01 mol), benzaldehydes (0.012 mol), 8 g alumina, and 4 g potassium hydroxide were homogenized in a mortar. Then, the mixture was irradiated in a reaction vessel of a CW-2000 focused microwave reactor

Scheme 1 Schematic representation of the synthesis and chemical structures of chalcones **2–9**

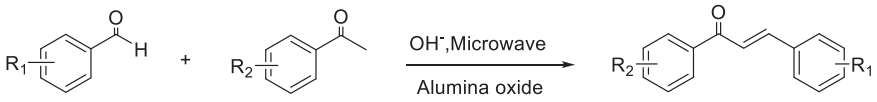

Scheme 2 Schematic representation of the synthesis and chemical structures of chalcones **1, 10–16**

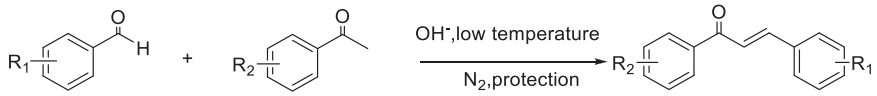

Scheme 3 Schematic representation of the synthesis and chemical structures of chalcones **17–31**

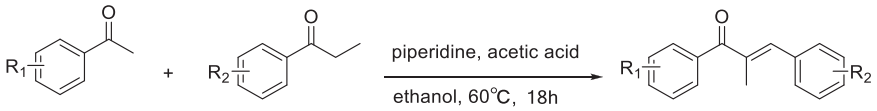

for 100 s after setting reaction power to 150 W. After cooling to room temperature, ice water (250 mL) was added to the reaction mixture and filtered through a general laboratory filter paper to separate the solid catalyst. Hydrochloric acid (2 mol L^{-1}) was added to the filtrate until the pH was 1–2 and the mixture was refrigerated at 4 °C for 20 min. The crude product was filtered and the residue was chromatographed on a flash silica-gel column using 25–50% EtOAc in hexane as the eluent.

*General methods for chalcones **1, 10–16***

The chalcones (**1**, **10–16)** were synthesized by the base catalyzed Claisen–Schmidt condensation reaction of the appropriately substituted acetophenones and aldehydes (Scheme 2).

Acetophenones (0.01 mol), benzaldehydes (0.012 mol) and absolute ethyl alcohol (32 mL) were stirred in a 250 mL three-necked flask at 0 °C for 1 h. A solution of potassium hydroxide (20 mmol) in a 4:1 (v/v) mixture of ethanol/H_2O (50 mL) was added into a flask containing N_2 and the resulting mixture was stirred at room temperature. The reaction was then monitored by TLC using ethyl acetate/petroleum ether (1:4 or 1:2 v/v) as the solvent system. The crude product was filtered and the residue was chromatographed on a flash silica-gel column using 25–50% EtOAc in hexane as eluent.

*General methods for chalcones **17–31***

The chalcones (**17–31**) were synthesized by the base catalyzed Claisen–Schmidt condensation reaction of the appropriately substituted acetophenones and aldehydes (Scheme 3).

A solution of 2,5-dimethoxypropiophenone (14.8 g, 0.076 mol), 4-(dimethy1amino) benzaldehyde (11.6 g, 0.078 mol), piperidine (15 mL), and acetic acid (7.5 mL) in ethanol (80 mL) was heated at reflux. After 18 h the solvent was removed and the residue was chromatographed on a flash silica-gel column using 25% EtOAc in hexane as eluant.

Characterization data

(E)-1,3-diphenyl-2-propen-1-one (compound **1**) Yellow solid (63.31%), m.p. 55.1–56.8 °C; ^{1}H NMR ($CDCl_3$, 600 MHz): δ 8.01–8.03 (m, 2H), 7.81 (d, $J = 15.98$ Hz, 1H), 7.63–7.65 (m, 2H), 7.55–7.60 (m, 2H), 7.48–7.52 (m, 2H), 7.39–7.42 (m, 3H); ^{13}C NMR ($CDCl_3$, 150 MHz): δ 190.52, 144.81, 138.16, 134.83, 132.76, 130.52, 128.93, 128.59, 128.47, 128.41, 122.02. MS: *m/e* 209 ($M + H^+$). Anal: $C_{15}H_{12}O$/208.

(E)-3-(2-hydroxyphenyl)-1-phenylprop-2-en-1-one (compound **2**) Light green solid (65.41%); m.p. 148.8–151.3 °C; ^{1}H NMR ($CDCl_3$, 600 MHz): δ 8.09 (d, $J = 16.05$ Hz, 1H), 7.97 (d, $J = 6.93$ Hz, 2H), 7.65 (d, $J = 16.05$ Hz, 1H), 7.51 (t, $J = 8.75$ Hz, 2H), 7.43 (t, $J = 8.39$ Hz, 2H), 7.23 (d, $J = 8.02$ Hz, 1H), 6.89 (t, $J = 8.02$ Hz, 1H), 6.84 (d, $J = 8.39$ Hz, 1H), 6.31 (bs, OH); ^{13}C NMR ($CDCl_3$, 150 MHz): δ 191.07, 155.62, 140.63, 138.36, 132.48, 131.81, 129.68, 128.68, 123.00, 122.34, 121.11, 116.63. MS: *m/e* 225 ($M + H^+$). Anal: $C_{15}H_{12}O_2$/224.

(*E*)-3-(3-hydroxyphenyl)-1-phenylprop-2-en-1-one (compound **3**) Yellow solid (70.45%); m.p. 223.4–224.6 °C; ^{1}H NMR ($CDCl_3$, 600 MHz): δ 8.01 (d, $J = 7.80$ Hz, 2H), 7.76 (d, $J = 15.61$ Hz, 1H), 7.58–7.61 (m, 1H), 7.51 (t, $J = 7.80$ Hz, 3H), 7.30 (t, $J = 7.80$ Hz, 1H), 7.22 (d, $J = 8.30$ Hz, 1H), 7.14 (s, 1H), 6.90–6.92 (m, 1H), 5.27 (bs, OH); ^{13}C NMR ($CDCl_3$, 150 MHz): δ 190.86, 155.98, 144.71, 138.08, 136.53, 133.02, 130.28, 128.76, 128.63, 122.49, 121.27, 117.82, 114.97. MS: *m/e* 225 ($M + H^+$). Anal: $C_{15}H_{12}O_2$/224.

(*E*)-3-(4-hydroxyphenyl)-1-phenylprop-2-en-1-one (compound **4**) Yellow solid (55.25%); m.p. 158.7–161.2 °C; ^{1}H NMR ($CDCl_3$, 600 MHz): δ 8.00 (d, $J = 7.08$ Hz, 2H),7.78 (d, $J = 15.45$ Hz, 1H), 7.55–7.59 (m, 3H), 7.50

(t, $J = 7.72$ Hz, 2H), 7.41 (d, $J = 15.45$ Hz, 1H), 6.89 (d, $J = 8.36$ Hz, 2H), 5.62 (bs, OH); ^{13}C NMR ($CDCl_3$, 150 MHz): δ 191.06, 158.20, 145.04, 138.99, 132.78, 130.66, 128.70, 128.55, 127,74, 119.83, 116.10. MS: *m/e* 225 ($M + H^+$). Anal: $C_{15}H_{12}O_2$/224.

(*E*)-1-(2,4-dihydroxyphenyl)-3-(4-hydroxyphenyl)prop-2-en-1-one (compound **5**) Yellow solid (58.90%), m.p. 198.1–199.7 °C; ^{1}H-NMR (DMSO, 600 MHz) δ: 6.26 (1H, d, $J = 1.8$ Hz, H-3′), 6.4 (1H, dd, $J = 1.8$ Hz, $J_1 = 8.4$ Hz, H-5′), 6.83(2H, d, $J = 9$ Hz, H-3, 5), 7.74 (1H, d, $J = 8.4$ Hz, H-6′), 7.78 (1H, d, $J = 15.2$ Hz, α-H), 7.85 (1H, d, $J = 15.2$ Hz, β-H), 8.15 (2H, d, $J = 9$ Hz, H-2, 6), 13.60 (1H, s, OH); ^{13}C-NMR (DMSO,150 MHz) δ: 193.4, 167.7, 166.7, 162.1, 146.1, 134.7, 133.1, 127.6, 119.3, 117.7, 114.8, 110.1, 104.5. MS: *m/e* 257 ($M + H^+$). Anal: $C_{15}H_{12}O_4$/256.

(*E*)-1-(2,4-dihydroxyphenyl)-3-(4-hydroxy-3-methoxyphenyl)prop-2-en-1-one (compound **6**) Yellow solid (57.60%), m.p. 206.7–209.6 °C; ^{1}H-NMR (DMSO, 600 MHz) δ: 3.87 (3H, s, OCH_3), 6.28 (1H, d, $J = 1.8$ Hz, H-2), 6.42 (1H, dd, $J_1 = 2.4$ Hz, $J_2 = 9.0$ Hz, H-5′), 6.78 (1H, d, $J = 8.4$ Hz, H-5), 7.28 (1H, dd, $J_1 = 1.8$ Hz, $J_2 = 8.4$ Hz, H-6), 7.54 (1H, d, $J = 2.4$ Hz, H-3′), 7.73 (1H, d, $J = 15$ Hz, H-α), 7.79 (1H, d, $J = 15$ Hz, H-β), 8.2 (1H, d, $J = 9.0$ Hz, H-6′), 13.65 (1H, s, OH); ^{13}C-NMR (DMSO, 150 MHz) δ: 193.4, 167.7, 166.8, 151.8, 149.9, 146.6, 134.7, 128.1, 57.5. MS: *m/e* 287 ($M + H^+$). Anal: $C_{16}H_{14}O_5$/286.

(*E*)-3-(3-hydroxy-4-methoxyphenyl)-1-(4-hydroxyphenyl) prop-2-en-1-one (compound **7**) Yellow solid (52.90%), m. p. 198.1–201.6 °C; ^{1}H-NMR (DMSO, 600 MHz) δ: 3.83 (3H, s, OCH_3), 6.82 (1H, d, $J = 1.8$ Hz, H-2), 6.88 (2H, d, $J = 9.0$ Hz, H-3′,5′), 6.98 (1H, d, $J = 9$ Hz, H-5), 7.26 (1H, dd, $J_1 = 1.8$ Hz, $J_2 = 9$ Hz, H-1,6), 7.55 (1H, d, $J = 15.6$ Hz, H-α), 7.65 (1H, d, $J = 15.6$ Hz, H-β), 8.03 (2H, d, $J = 8.4$ Hz, H-2′,6′), 9.13 (1H, s, OH-3), 10.36 (1H, s, OH-4′); ^{13}C-NMR (DMSO, 150 MHz) δ: 193.4, 164.0, 151.9, 148.5, 145.1, 133.1, 132.9, 131.3, 129.7, 126.81, 123.62, 121.3, 117.2, 113.8, 57.5. MS: *m/e* 271 ($M + H^+$). Anal: $C_{16}H_{14}O_4$/270.

(*E*)-1-(2,4-dihydroxyphenyl)-3-(3,4-dihydroxyphenyl)prop-2-en-1-one (compound **8**) Yellow solid (48.89%), m.p. 220.3–221.6 °C; ^{1}H-NMR (DMSO, 600 MHz) δ: 6.27 (1 H, d, $J = 2.4$ Hz, H-3′), 6.40 (1H, dd, $J_1 = 2.4$ Hz, $J_2 = 9$ Hz, H-5′), 6.81 (1H, d, $J = 8.4$ Hz, H-2), 7.20 (1H, dd, $J_1 = 1.8$ Hz, $J_2 = 8.2$ Hz, H-6), 7.37 (1H, d, $J = 1.8$ Hz, H-5), 7.65 (1H, d, $J = 15.3$ Hz, H-α), 7.71 (1H, d, $J = 15.3$ Hz, H-β), 8.14 (1H, d, $J = 9$ Hz, 6′), 13.60 (1H, s, OH); ^{13}C-NMR (DMSO, 150 MHz) δ: 193.3, 167.7, 166.8, 150.8, 147.5, 146.6, 134.7, 128.1, 124.3, 119.2, 117.7, 117.6, 114.9, 110.0, 104.5. MS: *m/e* 273 ($M + H^+$). Anal: $C_{15}H_{12}O_5$/272.

(*E*)-1,3-bis(4-hydroxyphenyl)prop-2-en-1-one (compound **9**) Yellow solid (38.75%), mp.196.2–198.4 °C; ^{1}H-NMR (DMSO, 600 MHz) δ: 6.82 (2H, d, $J = 8.4$ Hz, H-3, 5), 6.87 (3H, d, $J = 9$ Hz, H-3′, 5′), 7.61 (1H, d, $J = 15.6$ Hz, H-α), 7.68 (1H, d, $J = 15.6$ Hz, H-β), 7.70 (2H, d, $J = 8.4$ Hz, H-2, 6), 8.03 (3H, d, $J = 9$ Hz, H-2′, 6′), 10.03 (1H, s, OH), 10.34 (1H, s, OH); ^{13}C-NMR (DMSO, 150 MHz) δ: 188.9, 163.8, 161.7, 145.0, 132.8, 132.6, 127.9, 120.4, 117.6, 117.2. MS: *m/e* 241 ($M + H^+$). Anal: $C_{15}H_{12}O_3$/240.

(*E*)-1-(2,4-difluorophenyl)-3-(4-fluorophenyl)prop-2-en-1-one (compound **10**) Red solid (43.2%), m.p. 103.2–105.6 °C; ^{1}H-NMR (DMSO, 600 MHz) δ: 8.27 (2H, d, $J = 7.8$ Hz, H-2,6), 7.57 (2H, d, $J = 8.4$ Hz, H-3, 5), 7.48 (1H, d, $J = 15$ Hz, α-H), 7.75 (1H, d, $J = 15$ Hz, β-H), 6.24 ~ 7.25 (3H, m, ArH). ^{13}C-NMR (DMSO, 150 MHz) δ: 191.2, 164.2, 146.5, 144.1, 143.2, 140.3, 137.4, 133.1, 132.5, 129.0, 121.6, 112.5, 102.3. MS: *m/e* 263 ($M + H^+$). Anal: $C_{15}H_9F_3O$/262.

(*E*)-1-(2,4-dihydroxyphenyl)-3-(4-fluorophenyl)prop-2-en-1-one (compound **11**) Yellow solid (32.1%), m.p. 108.3–109.0 °C; ^{1}H-NMR (DMSO, 600 MHz) δ: 8.35 (2H, d, $J = 8.6$ Hz, H-2,6), 7.71 (2H, d, $J = 8.4$ Hz, H-3, 5), 7.51 (1H, d, $J = 15$ Hz, α-H), 7.79 (1H, d, $J = 15$ Hz, β-H), 6.25 ~ 7.67 (3H, m, Ar′H) 10.50(1H, s, OH-4′), 12.62(1H, s, OH-2′). ^{13}C-NMR (DMSO, 150 MHz) δ: 191.8, 169.2, 167.5, 164.9, 144.6, 132.5, 131.4, 120.6, 118.1, 116.1, 113.3, 108.1, 103.5. MS: *m/e* 259 ($M + H^+$). Anal: $C_{15}H_{11}FO_3$/258.

(*E*)-3-(4-fluorophenyl)-1-(4-hydroxyphenyl)prop-2-en-1-one (compound **12**) Yellow solid (36.0%), m.p. 104.7–105.4 °C; ^{1}H-NMR (DMSO, 600 MHz) δ: 8.31 (2H, d, $J = 8.6$ Hz, H-2,6), 7.70(2H, d, $J = 8.4$ Hz, H-3, 5), 7.67 (1H, d, $J = 15$ Hz, α-H), 7.82 (1H, d, $J = 15$ Hz, β-H), 7.91 (2H, d, $J = 8.7$ Hz, H-3′, 5′), 8.40 (2H, d, $J = 8.4$ Hz, H-2′,6′), 10.54 (1H, s, OH-4′). ^{13}C-NMR (DMSO, 150 MHz) δ: 193.5, 170.5, 167.3, 145.4, 141.2,123.1, 129.6, 120.5, 115.6, 114.6, 101.6. MS: *m/e* 243 ($M + H^+$). Anal: $C_{15}H_{11}FO_2$/242.

(*E*)-3-(4-fluorophenyl)-1-(2-hydroxyphenyl)prop-2-en-1-one (compound **13**) Yellow solid (48.9%), m.p. 105.8–106.9 °C; ^{1}H-NMR (DMSO, 600 MHz) δ: 8.35 (2 H, d, $J = 8.6$ Hz, H-2,6), 7.71 (2H, d, $J = 8.4$ Hz, H-3, 5), 7.64 (1H, d, $J = 15$ Hz, α-H), 8.13 (1H, d, $J = 15$ Hz, β-H), 6.30 ~ 7.65 (3H, m, Ar'H), 12.74 (1H, s, OH-2′). ^{13}C-NMR (DMSO, 150 MHz) δ: 194.1, 169.1, 165.7, 145.7, 131.7, 131.5, 129.6, 121.6, 120.6, 115.9, 112.5, 110.4, 107.5. MS: *m/e* 243 ($M + H^+$). Anal: $C_{15}H_{11}FO_2$/242.

(*E*)-1-(2,4-difluorophenyl)-3-(4-hydroxyphenyl)prop-2-en-1-one (compound **14**) Yellow solid (35.4%), m.p.

104.6–106.7 °C; ^{1}H-NMR (DMSO, 600 MHz) δ: 8.31 (2H, d, $J = 8.6$ Hz, H-2′,6′), 7.70 (2H, d, $J = 8.4$ Hz, H-3′, 5′), 7.67 (1H, d, $J = 15$ Hz, α-H), 7.82 (1H, d, $J = 15$ Hz, β-H), 6.60 ~ 7.65 (3H, m, ArH), 10.03 (1H, s, OH-4). ^{13}C-NMR (DMSO, 150 MHz) δ: 194.7, 171.6, 169.9, 169.1, 149.5, 146.3, 124.7, 123.6, 126.8, 119.5, 112.1, 110.5, 105.7. MS: *m/e* 261 ($M + H^+$). Anal: $C_{15}H_{10}F_2O_2$/260.

(*E*)-1-(2,4-difluorophenyl)-3-(4-hydroxy-3-methoxyphenyl) prop-2-en-1-one (compound **15**) Yellow solid (26.4%), m. p. 110.3–111.5 °C; ^{1}H-NMR (DMSO, 600 MHz) δ: 3.37 (3H, s, OCH_3), 6.43 ~ 6.65 (3H, m, ArH), 6.20 ~ 7.65 (3H, m, Ar′H), 10.54 (1H, s, OH). ^{13}C-NMR (DMSO, 150 MHz) δ: 196.1, 163.5, 162.4, 161.7, 159.7, 149.5, 132.5, 132.1, 127.8, 124.5, 116.8, 116.3, 110.5, 103.7, 102.5. 55.9. MS: *m/e* 291 ($M + H^+$). Anal: $C_{16}H_{12}F_2O_3$/290.

(*E*)-1-(2,4-difluorophenyl)-3-(3-hydroxy-4-methoxyphenyl) prop-2-en-1-one (compound **16**) Yellow solid (40.3%), m. p. 110.7–112.0 °C; ^{1}H-NMR (DMSO, 600 MHz) δ: 3.74 (3H, s, OCH_3), 6.45 ~ 6.75 (3H, m, ArH), 6.61 ~ 7.47 (3H, m, Ar'H), 10.09 (1H, s, OH). ^{13}C-NMR (DMSO, 150 MHz) δ: 197.5, 163.7, 163.4, 159.7, 157.7, 149.6, 132.6, 131.2, 127.7, 124.5, 116.8, 116.1, 110.5, 102.7, 101.5. 55.5. MS: *m/e* 291 ($M + H^+$). Anal: $C_{16}H_{12}F_2O_3$/290.

(*E*)-1-(2,4-dihydroxyphenyl)-2-methyl-3-(4-nitrophenyl) prop-2-en-1-one (compound **17**) Yellow solid (40.3%), m. p. 162.7–164.1.0 °C; ^{1}H-NMR (DMSO, 600 MHz) δ: 13.1 (s, OH), 8.10 (d, $J = 8.8$ Hz, H), 7.82(s, H), 7.73 (d, $J = 8.8$ Hz, 2H), 6.92 (d, $J = 8.8$ Hz, 2H), 6.46 (dd, $J = 8.8$ Hz, 2.0 Hz, 6.36 (d, $J = 2.0$ Hz, H), 2.25 (brs, 3H). ^{13}C-NMR (DMSO, 150 MHz) δ: 192.3, 167.6, 165.6, 145.7, 133.1, 132.1, 129.0, 128.6, 118.6, 114.5, 112.5, 108.7, 103.7, 22.5. MS: *m/e* 300 ($M + H^+$). Anal: $C_{16}H_{13}NO_5$/299.

(*E*)-1-(2,4-dihydroxyphenyl)-3-(4-fluorophenyl)-2-methyl-prop-2-en-1-one (compound **18**) Yellow solid (55.3%), m. p. 176.7–178.1.0 °C; ^{1}H-NMR (DMSO, 600 MHz) δ: 13.6 (s, OH), 8.33 (d, $J = 9.0$ Hz, 2H), 7.83 (d, $J = 9.0$ Hz, H), 7.71 (d, $J = 9.0$ Hz, 2H), 7.58 (s, H), 5.97 (dd, $J = 9.0$ Hz, 2.0 Hz, H), 2.13 (brs, 3H). ^{13}C-NMR (DMSO, 150 MHz) δ: 189.7, 173.8, 170.5, 136.9, 135.3, 133.6, 130.6, 127.5, 115.8, 111.9, 110.5, 105.8, 100.1, 25.6. MS: *m/e* 273 ($M + H^+$). Anal: $C_{16}H_{13}FO_3$/272.

(*E*)-1-(2,4-dihydroxyphenyl)-3-(4-(dimethylamino)phenyl)-2-methylprop-2-en-1-one (compound **19**) Yellow solid (55.3%), m.p. 89.3–91.8 °C; ^{1}H-NMR (DMSO, 600 MHz) δ: 12.,15 (s, OH), 7.9 (s, H), 7.65 (d, $J = 8.6$ Hz, H), 6.93 (s, H), 6.83 (d, $J = 8.6$ Hz, 2H), 6.50 (dd, $J = 8.6$ Hz, 2.2 Hz, H), 6.21 (d, $J = 2.2$ Hz, H), 2.91 (s, 6H), 2.36 (brs, 3H). ^{13}C-NMR (DMSO, 150 MHz) δ: 187.5, 172.3, 159.8, 153.7, 131.9, 130.2, 127.1, 125.5, 120.3, 113.6, 109.8, 105.6, 105.3, 40.7, 27.3. MS: *m/e* 298 ($M + H^+$). Anal: $C_{18}H_{19}NO_3$/297.

(*E*)-1-(2,4-dihydroxyphenyl)-2-methyl-3-phenylprop-2-en-1-one (compound **20**) Yellow solid (65.4%), m.p. 113.3–114.8 °C; ^{1}H-NMR (DMSO, 600 MHz) δ: 12.5 (s, OH), 7.5 (d, $J = 8.7$ Hz, H), 7.38–7.34 (m, 4H), 7.21 (s, H), 6.96 (d, $J = 16.1$ Hz), 6.85 (dd, $J = 8.7$ Hz, 2.6 Hz, H), 6.5 (d, $J = 2.6$ Hz), 1.83 (brs, 3H). ^{13}C-NMR (DMSO, 150 MHz) δ: 189.5, 170.1, 163.2, 148.6, 129.8, 129.1, 128.8, 128.4, 126.9, 115.7, 114.7, 104.9, 103.8, 28.4. MS: *m/e* 255 ($M + H^+$). Anal: $C_{16}H_{14}O_3$/254.

(*E*)-1-(2,4-dihydroxyphenyl)-3-(4-hydroxyphenyl)-2-methylprop-2-en-1-one (compound **21**) Yellow solid (67.4%), m.p. 103.3–104.9 °C; ^{1}H-NMR (DMSO, 600 MHz) δ: 7.92 (d, $J = 8.5$ Hz, H), 7.83 (d, $J = 7.0$ Hz,2H), 7.21 (s, H), 6.89 (d, $J = 8.32$ Hz, 2H), 6.40 (dd, $J = 8.5$ Hz, 2.4 Hz, H), 6.32 (d, $J = 2.4$ Hz, H), 5.32 (brs, H), 2.65 (d, J = Hz). ^{13}C-NMR (DMSO, 150 MHz) δ: 191.5, 172.3, 170.5, 149.8, 130.5, 130.1, 128.6, 127.5, 120.4, 113.6, 112.7, 109.2, 105.9, 25.1. MS: *m/e* 271 ($M + H^+$). Anal: $C_{16}H_{14}O_4$/270.

(E)-2-methyl-3-(4-nitrophenyl)-1-phenylprop-2-en-1-one (compound **22**) Yellow solid (77.4%), m.p. 103.3–104.9 °C; ^{1}H-NMR (DMSO, 600 MHz) δ: 8.00 (d, $J = 7.08$ Hz, 2H), 7.78 (s, H), 7.55–7.59 (m, 3H), 7.50 (t, $J = 7.72$ Hz, 2H), 6.89 (d, $J = 8.36$ Hz, 2H). 2.67 (brs, 3H). ^{13}C-NMR (DMSO, 150 MHz) δ: 185.6, 158.2, 132.7, 131.8, 131.6, 130.5, 128.7, 127.8, 119.6, 116.2, 110.5, 29.6. MS: *m/e* 268 ($M + H^+$). Anal: $C_{16}H_{13}NO_3$/267.

(*E*)-3-(4-fluorophenyl)-2-methyl-1-phenylprop-2-en-1-one (compound **23**) Yellow solid (59.4%), m.p. 100.3–102.9 °C; ^{1}H-NMR (DMSO, 600 MHz) δ: 7.93(d, $J = 7.1$ Hz, 2H), 7.6 (s, H), 7.50–7.63 (m, 3H), 7.4 (t, $J = 7.2$, 2H), 6.75 (d, $J = 8.21$ Hz, 2H), 2.81 (s, 6H), 2.32 (brs, 3H). ^{13}C-NMR (DMSO, 150 MHz) δ: 193.5, 149.8, 133.6, 132.1, 130.7, 129.5, 128.6, 126.4, 120.1, 116.3, 111.5, 21.6. MS: *m/e* 241 ($M + H^+$). Anal: $C_{16}H_{13}FO$/240.

(*E*)-3-(4-(dimethylamino)phenyl)-2-methyl-1-phenylprop-2-en-1-one (compound **24**) Yellow solid (56.4%), m.p. 85.3–87.9 °C; ^{1}H-NMR (DMSO, 600 MHz) δ: 8.01 (d, $J = 6.9$ Hz, 2H), 7.8 (s, H), 7.2–7.5 (m, 3H), 6.9 (t, $J = 7.0$ Hz, 2H), 6.52 (d, $J = 7.9$ Hz, 2H), 2.50 (brs, 3H). ^{13}C-NMR (DMSO, 150 MHz) δ: 182.1, 149.6, 134.8, 133.7, 131.1, 129.6, 126.3, 124.9, 120.7, 115.6, 108.9, 41.8, 28.6. MS: *m/e* 266 ($M + H^+$). Anal: $C_{16}H_{13}NO$/265.

(*E*)-2-methyl-1,3-diphenylprop-2-en-1-one(compound **25**) Yellow solid (66.4%), m.p. 115.3–117.9 °C; ^{1}H-NMR (DMSO, 600 MHz) δ: 8.01–8.03 (m, 2H), 7.81 (s, 1H), 7.63–7.65 (m, 2H), 7.55–7.60 (m, 2H), 7.48–7.52 (m, 2H), 7.39–7.42 (m, 2H), 2.31 (brs, 3H). ^{13}C NMR (DMSO, 150 MHz): δ 190.52, 144.81, 138.16, 134.83, 132.76,130.52, 128.93, 128.59, 128.47, 128.41, 122.02, 27.8. MS: *m/e* 223 ($M + H^+$). Anal: $C_{16}H_{14}O$/222.

(*E*)-3-(4-hydroxyphenyl)-2-methyl-1-phenylprop-2-en-1-one(compound **26**) Yellow solid (66.4%), m.p. 95.2–97.8 °C; ^{1}H-NMR (DMSO, 600 MHz) δ: 8.02 (d, $J = 7.3$ Hz, 2H), 7.91 (t, $J = 7.3$ Hz, 2H), 7.42–7.86 (m, 3H), 7.01 (s, H), 6.73 (d, $J = 8.0$ Hz, 2H), 2.42 (brs, 3H). ^{13}C NMR (DMSO, 150 MHz): δ 190.2, 149.8, 135.6, 134.2, 133.8, 130.6, 128.1, 127.9, 120.1, 115.8, 110.6, 22.3. MS: *m/e* 239 ($M + H^+$). Anal: $C_{16}H_{14}O_2$/238.

(*E*)-1-(4-hydroxyphenyl)-2-methyl-3-(4-nitrophenyl)prop-2-en-1-one (compound **27**) Yellow solid (26.4%), m.p. 91.3–93.9 °C; ^{1}H-NMR (DMSO, 600 MHz) δ: 8.04 (d, $J = 8.8$ Hz, 2H), 7.95 (s, H), 7.70 (d, $J = 8.6$ Hz, 2H), 7.56 (d, $J = 8.3$ Hz, 2H), 7.01 (d, $J = 8.6$ Hz, 2H), 6.83 (d, $J = 9.3$ Hz, 2H), 6.02 (d, $J = 9.0$ Hz, 2H), 5.409 (s, OH), 2.56 (brs, 3H). ^{13}C NMR (DMSO,150 MHz): δ 190.5, 161.6, 150.8, 132.8, 131.2, 129.0, 119.2, 115.3, 24.7. MS: *m/e* 284 ($M + H^+$). Anal: $C_{16}H_{13}NO_4$/283.

(*E*)-3-(4-fluorophenyl)-1-(4-hydroxyphenyl)-2-methylprop-2-en-1-one (compound **28**) Yellow solid (86.3%), m.p. 90.3–92.9 °C; ^{1}H-NMR (DMSO, 600 MHz): δ 8.60 (d, $J = 7.6$ Hz, 2H), 8.24 (s, H), 7.92 (d, $J = 9.1$ Hz, 2H), 6.52 (d, $J = 8.2$ Hz, 2H), 5.64 (d, $J = 9.1$ Hz, 2H), 2.35 (brs, 3H). ^{13}C NMR (DMSO,150 MHz):δ: 193.1, 165.8, 153.2, 132.7, 130.5, 129.6, 128.6, 123.9, 120.5, 117.8, 112.4, 26.5. MS: *m/e* 257 ($M + H^+$). Anal: $C_{16}H_{13}FO_2$/256.

(*E*)-3-(4-(dimethylamino)phenyl)-1-(4-hydroxyphenyl)-2-methylprop-2-en-1-one (compound **29**) Yellow solid (62.3%), m.p. 121.3–122.9 °C; ^{1}H-NMR (DMSO, 600 MHz): δ 8.50 (d, $J = 7.9$ Hz, 2H), 8.34 (s, H), 8.02 (d, $J = 8.6$ Hz, 2H), 6.53 (d, $J = 8.2$ Hz, 2H), 2.98 (brs, 3H), 2.54 (s, 6H). ^{13}C NMR (DMSO,150 MHz) δ: 187.6, 165.9, 154.9, 133.1, 130.5, 128.7, 127.5, 124.6, 121.7, 118.2, 107.8, 45.6, 25.7. MS: *m/e* 282 ($M + H^+$). Anal: $C_{18}H_{19}NO_2$/281.

(*E*)-1-(4-hydroxyphenyl)-2-methyl-3-phenylprop-2-en-1-one(compound **30**) Yellow solid (62.3%), m.p. 92.1–92.9 °C; ^{1}H-NMR (DMSO, 600 MHz): δ 8.51 (d, $J = 8.3$ Hz, 2H), 8.3 (s, H), 8.15 (d, $J = 8.1$ Hz, 2H), 6.49 (d, $J = 8.2$ Hz, 2H), 5.3 (d, $J = 8.2$ Hz, 2H), 2.65 (brs, 3H). ^{13}C NMR (DMSO,150 MHz) δ: 191.6, 167.2, 159.7, 133.8, 129.1, 126.9, 121.9, 120.1, 27.8. MS: *m/e* 239 ($M + H^+$). Anal: $C_{14}H_{16}O_2$/238.

(*E*)-1,3-bis(4-hydroxyphenyl)-2-methylprop-2-en-1-one (compound **31**) Yellow solid (43.3%), m.p. 123.1–124.9 °C; ^{1}H-NMR (DMSO, 600 MHz): δ 8.30 (d, $J = 8.7$ Hz, 2H), 8.21 (s, H), 8.02 (d, $J = 7.3$Hz, 2H), 6.73 (d, $J = 8.0$, 2H), 5.6 (d, $J = 8.6$ Hz, 2H), 2.76 (brs, 3H). ^{13}C NMR (DMSO, 150 MHz) δ: 187.5, 169.2, 158.6, 135.6, 132.7, 131.6, 129.3, 127.3, 121.8, 121.5, 110.8, 26.3. MS: *m/e* 255 ($M + H^+$). Anal: $C_{16}H_{14}O_3$/254.

Biological

Cell culture

HeLa, SiHa, and CHO cells were grown in Dulbecco's Modified Eagle Media. The media were supplemented with 100 U/mL penicillin, 100 mg/mL streptomycin and 10% fetal bovine serum. Cells were incubated at 37 °C in a humidified atmosphere containing 5% CO_2.

In vitro anti-proliferative assay

Cells were seeded into 96-well plates (5000 cells/well) and incubated at 37 °C in a humidified 5% CO_2 atmosphere. After 24 h, the cells were treated with different concentrations of the compounds. Concentrated (5 mg) solutions of chalcones were prepared in DMSO. Cell viability after 24, 48, and 72 h of drug exposure was determined using the MTT cell viability assay, as described previously.

Apoptosis assay

The SiHa and HeLa cells were treated with various concentrations (0, 1, 2, 4 $\mu g\,mL^{-1}$) of compound **19** for 24 h and then stained with both Annexin V-FITC and PI 50. Then samples were analyzed with an EPICS XL/XL-MCL flow cytometer (USA Beckmann).

Docking simulation

The molecule was docked to the crystal structure of the yeast 20S proteasome in complex with the inhibitor homobelactosin C covalently bound to the terminal threonine of the β5 active site [PDB code: 3E47]. The structures were retrieved from the PDB archive (www.pdb.org), and the docking simulation has been performed using the MOE/Dock procedure integrated in the AutoDock Tools 1.5.6 system of programs (Chemical Computing Group). During the first step of the docking application, the ligand was treated in a flexible manner by rotating routable bonds. Several configurations were generated and scored in an

effort to determine favorable binding modes by the application of the R triangle placement method. The ligand was docked, restricting the search for binding modes to a specific, small region of the subunit called the β5-binding site, in which the terminal Thr1 is the active residue.

Acknowledgements This research work was financially supported by Natural National Science Foundation of China (81260379). We would like to thank Professor Mourboul for helping us with the synthesis, biological evaluation and English language editing.

Compliance with ethical standards

Conflict of interest The authors declare that they have no competing interests.

References

Ahmad S, Israf DA, Lajis NH, Shaari K, Mohamed H, Wahab A, Ariffin KT, Hoo WY, Aziz NA, Kadir AA (2006) Cardamonin, inhibits pro-inflammatory mediators in activated RAW 264.7 cells and whole blood. Eur J Pharmacol 538:188–194

Ahmed Belkacem A, Pozza A, Macalou S, Pérez-Victoria JM, Boumendjel A, Di PA (2006) Inhibitors of cancer cell multidrug resistance mediated by breast cancer resistance protein (BCRP/ABCG2). Anti-cancer Drugs 17:239–243

Bazzaro M, Anchoori RK, Mudiam MK, Issaenko O, Kumar S, Karanam B, Lin ZH, Vogel RI, Gavioli R, Destro F, Ferretti V, Roden RB, Khan SR (2011) α,β-Unsaturated carbonyl system of chalcone-based derivatives is responsible for broad inhibition of proteasomal activity and preferential killing of human papilloma virus (HPV) positive cervical cancer cells. J Med Chem 54:449

Bazzaro M, Lin Z, Santillan A, Lee K, Wang M, Chan C, Bristow E, Mazitschek R, Bradner J, Roden B (2008) Ubiquitin proteasome system stress underlies synergistic killing of ovarian cancer cells by bortezomib and a novel HDAC6 inhibitor. Clin Cancer Res 14:7340–7347

Bois F, Beney C, Boumendjel A, Mariotte AM, Conseil G, Di Pietro A (1998) Halogenated chalcones with high-affinity binding to P-glycoprotein: potential modulators of multidrug resistance. J Med Chem 41:4161–4164

Bois F, Boumendjel A, Mariotte A, Conseil G, Di Petro A (1999) Synthesis and biological activity of 4-alkoxy chalcones: potential hydrophobic modulators of P-glycoprotein-mediated multidrug resistance. Bioorg Med Chem 7:2691–2695

Brannigan JA, Dodson G, Duggleby HJ, Moody PC, Smith JL, Tomchick DR, Murzin AG (1995) A protein catalytic framework with an N-terminal nucleophile is capable of self-activation. Nature 378:416–419

Chimenti F, Bizzarri B, Manna F, Bolasco A, Secci D, Chimenti P, Granese A, Rivanera D, Lilli D, Scaltrito MM, Brenciaglia MI (2005) Synthesis and in vitro selective anti-Helicobacter pylori activity of pyrazoline derivatives. Bioorg Med Chem Lett 15:603–607

Ciechanover A (1993) The ubiquitin-mediated proteolytic pathway. Brain Pathol 3:67–75

Ciechanover A, Finley D, Varshavsky A (1984) The ubiquitin-mediated proteolytic pathway and mechanisms of energy-dependent intracellular protein degradation. J Cell Biochem 24:27–53

Climent MJ, Garcia H, Primo J, Corma A (1990) Zeolites as catalysts in organic reactions. Claisen-Schmidt condensation of acetophenone with benzaldehyde. Catal Lett 4:85–91

Deka N, Sarma JC (2001) Microwave-mediated selective monotetrahydropyranylation of symmetrical diols catalyzed by iodine. J Org Chem 66:1947–1948

Dimmock JR, Elias DW, Beazely MA, Kandepu NM (1999) Bioactivities of chalcones. Curr Med Chem 6:1125

Dimmock JR, Jha A, Zello GA, Allen TM, Santos CL, Balzarini J, De Clercq E, Manavathu EK, Stables JP (2003) Cytotoxic 4'-aminochalcones and related compounds. Pharmazie 34:227

Ducki S, Forrest R, Hadfield JA, Kendall A, Lawrence NJ, McGown AT, Rennison D (1998) Potent antimitotic and cell growth inhibitory properties of substituted chalcones. Bioorg Med Chem Lett 8:1051–1056

Groll M, Oleg V, Huber R, Meijere A (2006) Inhibitor-binding mode of homobelactosin C to proteasomes: new insights into class I MHC ligand generation. PNAS 3:4576–4579

Hsu YL, Kuo PL, Tzeng WS, Lin CC (2006) Chalcone inhibits the proliferation of human breast cancer cell by blocking cell cycle progression and inducing apoptosis. Food Chem Toxicol 44:704–713

Iranpoor N, Kazemi F (1998) $RuCl_3$ catalyses aldol condensations of aldehydes and ketones. Tetrahedron 54:9475–9480

Kalita DJ, Borah R, Sarma JC (1999) A selective catalytic method of enolacetylation under microwave Irradiation. J Chem Res 999:404–405

Lawrence NJ, McGown AT (2005) The chemistry and biology of antimitotic chalcones and related enone systems. Curr Pharm Des 11:1679–1693

Lawrence NJ, Patterson RP, Ooi LL, Cook D, Ducki S (2006) Effects of α-substitutions on structure and biological activity of anticancer chalcones. Bioorg Med Chem Let 16:5844–5848

Lee JS, Paull K, Alvarez M, Hose C, Monks A, Grever M, Fojo AT, Bates SE (1994) Rhodamine efflux patterns predict P-glycoprotein substrates in the National cancer institute drug screen. Mol Pharmacol 46:627–638

Leong CO, Suggitt M, Swaine DJ, Bibby MC, Stevens MF, Bradshaw TD (2005) In vitro, in vivo, and in silico analyses of the antitumor activity of 2-(4-amino-3-methylphenyl)-5-fluorobenzothiazoles. Mol Cancer Therap 3:1565–1575

Leong CO, Vidnovic N, Deyoung MP, Sgroi D, Ellisen LW (2007) The p63/p73 network mediates chemosensitivity to cisplatin in a biologically defined subset of primary breast cancers. J Clin Invest 117:1370–1380

Liu X, Go ML (2006) Antiproliferative properties of piperidinylchalcones. Bioorg Med Chem 14:153–163

Liu XL, Tee HW, Go ML (2008) Functionalized chalcones as selective inhibitors of P-glycoprotein and breast cancer resistance protein. Bioorg Med Chem 16:171–180

Löwe J, Stock D, Bing J, Zwickl P, Baumeister W, Huber R (1995) Crystal structure of the 20S proteasome from the archaeon T. acidophilum at 3.4Å resolution. Science 268:533–539

Ni L, Meng CQ, Sikorski JA (2005) Recent advances in therapeutic chalcones. Expert Opin Ther Pat 14:1669–1691

Pati HN, Holt HL, LeBlanc R, Dickson J, Stewart M, Brown T, Lee M (2005) Synthesis and cytotoxic properties of nitro-and amino-chalcones. Med Chem Res 14:19–25

Petrov O, Ivanova Y, Gerova M (2008) SOCl2/EtOH: catalytic system for synthesis of chalcones. Catal Commun 9:315–316

Robert J, Jarry C (2003) Multidrug resistance reversal agents. J Med Chem 46:4805–4817

Rocco JW, Leong CO, Kuperwasser N, DeYoung MP, Ellisen LW (2006) p63 mediates survival in squamous cell carcinoma by suppression of p73-dependent apoptosis. Cancer Cell 9:45–56

Romagnoli R, Baraldi PG, Carrion MD, Cruz-Lopez O, Cara CL, Balzarini J, Hamel E, Canella A, Fabbri E, Gambari R, Basso G, Viola G (2009) Hybrid α-bromoacryloylamido chalcones. Design, synthesis and biological evaluation. Bioorg Med Chem Lett 19:2022–2028

Saikia M, Kakati D, Joseph MS, Sarma JC (2009) Iodine-alumina catalyzed Aza- Michael addition under solvent free conditions. Lett Org Chem 6:654–658

Seelig A, Landwojtowicz E (2000) Structure-activity relationship of P-glycoprotein substrates and modifiers. Eur J Pharm Sci 12:31–40

Sogawa S, Nihro Y, Ueda H, Izumi A, Miki T, Matsumoto H, Satoh T (1993) 3,4-Dihydroxychalcones as potent 5-lipoxygenase and cyclooxygenase inhibitors. J Med Chem 36:3904–3909

Tanaka k (2009) The proteasome: overview of structure and functions. Proc Jpn Acad Ser B 85:12–36

Valla A, Valla B, Cartier D, Le Guillou R, Labia R, Florent L, Charneau S, Schrevel J, Potier P (2006) New syntheses and potential antimalarial activities of new 'retinoid-like chalcones. Eur J Med Chem 41:142–146

Xia Y, Yang ZY, Xia P, Bastow KF, Nakanishi Y, Lee KH (2000) Antitumor agents. Part 202: novel 2'-amino chalcones: design, synthesis and biological evaluation. Bioorg Med Chem Lett 10:699–701

Zamora JM, Pearce HL, Beck WT (1988) Physical-chemical properties shared by compounds that modulate multidrug resistance in human leukemic cells. Mol Pharmacol 33:454–462

Zhao LM, Jin HS, Sun LP, Piao HR, Quan ZS (2005) Synthesis and evaluation of antiplatelet activity of trihydroxychalcone derivatives. Med Chem Lett 15:5027–5029